

**Long-term, on-line monitoring of microbial  
biofilms using a quartz crystal microbalance**

David E. Nivens, James Q. Chambers, Tina R. Anderson, and David C. White

*Anal. Chem.*, **1993**, 65 (1), 65-69 • DOI: 10.1021/ac00049a013 • Publication Date (Web): 01 May 2002

Downloaded from <http://pubs.acs.org> on February 12, 2009

**More About This Article**

---

The permalink <http://dx.doi.org/10.1021/ac00049a013> provides access to:

- Links to articles and content related to this article
- Copyright permission to reproduce figures and/or text from this article



# Long-Term, On-Line Monitoring of Microbial Biofilms Using a Quartz Crystal Microbalance

David E. Nivens,\*†‡ James Q. Chambers,† Tina R. Anderson,† and David C. White\*‡§

Department of Chemistry and Center for Environmental Biotechnology, University of Tennessee, Knoxville, Tennessee 37932, and Environmental Science Division, Oak Ridge National Laboratory, Oak Ridge, Tennessee 37831

A quartz crystal microbalance was used to nondestructively monitor the formation of *Pseudomonas cepacia* biofilms. These experiments involved long-term monitoring over days. Long-term monitoring initially encountered problems associated with baseline drift which were not observed in short-term electrochemical experiments or studies performed in vacuum or air. The extent of baseline drift produced by fluctuations in hydrostatic pressure and temperature was ascertained. Results showed that 5-MHz AT-cut quartz crystals sealed into flow cells and exposed to aqueous environments were more sensitive to pressure and temperature changes than crystals exposed to air. A test system was designed to eliminate these interferences in order to monitor the frequency shift caused by the attachment and surface growth of *P. cepacia* cells. A calibration curve for the frequency shift corresponding to a given number of bacteria within a biofilm was generated, and the detection limit of the technique was determined to be  $3 \times 10^5$  cells-cm<sup>-2</sup>. The calibration curve was utilized to produce graphs of the number of attached cells versus time, and the first derivative curves were used to study rates of biofilm formation.

## INTRODUCTION

Microorganisms are ubiquitous in most aqueous environments. Many of these microbes, which are present in aqueous systems such as lakes, oceans, municipal and industrial water systems, and even reagent bottles on laboratory benches, have a peculiar *modus operandi* in which they attach to surfaces and form gelatinous films termed biofilms. The literature on biofilms and biofilm processes has been extensively reviewed.<sup>1-3</sup> Biofilms are dynamic by nature and can influence interfacial, liquid phase, and surface chemistry. For instance, biofilms degrade waste in water treatment plants,<sup>4</sup> reduce heat transfer in heat-exchange units,<sup>5</sup> are a source of chemical as well as microbial contamination in water systems,<sup>6</sup> and facilitate corrosion of metal structures.<sup>7</sup> In medicine, biofouling has been implicated in the failure of implanted devices

such as catheters,<sup>8</sup> voice prostheses,<sup>9</sup> and endocardial pacemakers.<sup>10</sup>

Classical microbiological studies of biofilms involve methods that require the removal of the sample from its aqueous environment and subsequent microscopic, microbiological, or biochemical analyses. These off-line methodologies are plagued with problems resulting from sample removal and/or rinsing procedures that can alter or damage the biofilms. In addition, off-line methods are notoriously labor-intensive and do not provide instantaneous feedback. Therefore, microbiologists and microbial ecologists covet techniques that can provide in situ data on the formation of microbial biofilms.

On-line detection of developing biofilms has been accomplished with both microscopic and analytical techniques. Originally, microscopic techniques utilized time-lapsed videotape to record phase-contrast images of bacteria attaching to cellulose membranes.<sup>11</sup> Scanning confocal laser microscopy increased the resolution of the images and generated excellent three-dimensional views of biofilms.<sup>12</sup> Attenuated total reflection Fourier transform infrared spectroscopy provided molecular details about the inner portion of biofilms by generating infrared absorption spectra from bacteria located approximately 1  $\mu$ m from the surface of germanium crystals.<sup>13</sup>

The quartz crystal microbalance (QCM) is used to examine interfacial phenomena and study the formation of abiotic polymer films. This technique utilizes an AT-cut quartz crystal, a broad-band oscillator, and a frequency counter to monitor mass changes on the quartz resonator. Reviews of the QCM technique have been published.<sup>14-16</sup> In biological systems, the QCM technique detected adenosine 5'-phosphosulfate reductase and human chorionic gonadotropin<sup>17</sup> and indirectly detected microorganisms in the liquid phase by monitoring metabolite production.<sup>18</sup> However, little attention has been given to use of the QCM for long-term monitoring in aqueous environments.

In the study described herein, the QCM was employed to monitor the attachment and surface growth of the bacterium

\* Corresponding author: David E. Nivens, Center for Environmental Biotechnology, 10515 Research Drive, Building 1, Suite 300, Knoxville, TN 37932.

† Department of Chemistry, University of Tennessee.

‡ Center for Environmental Biotechnology, University of Tennessee.

§ Environmental Science Division, ORNL.

(1) *Adsorption of Microorganisms to Surfaces*; Marshall, K. C., Bitton, G., Eds.; John Wiley & Sons: New York, 1980.

(2) *Structure and Function of Biofilms*; Characklis, W. G., Wilderer, P. A., Eds.; John Wiley & Sons: New York, 1989.

(3) *Biofilms*; Characklis, W. G., Marshall, K. C., Eds.; John Wiley & Sons: New York, 1990.

(4) Bryers, J. D.; Characklis, W. G. In *Biofilms*; Characklis, W. G., Marshall, K. C., Eds.; John Wiley and Sons: New York, 1990; pp 671-696.

(5) Characklis, W. G. In *Biofilms*; Characklis, W. G., Marshall, K. C., Eds.; John Wiley & Sons: New York, 1990; pp 523-584.

(6) Patterson, M. K.; Husted, G. R.; Rutkowski, A.; Mayette, D. C. *Ultrapure Water* 1991, 8, 18.

(7) *Microbially Influenced Corrosion and Biodeterioration*; Dowling, N. J., Mittelman, M. W., Danko, J. C., Eds.; The University of Tennessee Press: Knoxville, 1990.

(8) Mahieu, H. F.; van Saene, H. K. F.; Rosingh, H. J.; Schutte, H. K. *Arch. Otolaryngol., Head Neck Surg.* 1986, 112, 321-228.

(9) Marrie, T. J.; Nelligan, J.; Costerton, J. W. *Circulation* 1982, 66, 1339-1346.

(10) Marrie, T. J.; Noble, M. N.; Costerton, J. W. *J. Clin. Microbiol.* 1983, 18, 1388-98.

(11) Kjelleberg, S.; Humphrey, B. A.; Marshall, K. C. *Appl. Environ. Microbiol.* 1982, 43, 1166.

(12) Lawrence, J. R.; Korber, D. R.; Hoyle, B. D.; Costerton, J. W.; Caldwell, D. E. *J. Bacteriol.* 1991, 173, 6558-6567.

(13) Nivens, D. E.; Chambers, J. Q.; Anderson, T. R.; Tunlid, A.; Smit, J.; White, D. C. *J. Microbiol. Methods*, in press.

(14) Deakin, M. R.; Buttry, D. A. *Anal. Chem.* 1989, 61, 1147A-1154A.

(15) Suhumacher, R. *Angew. Chem., Int. Ed. Engl.* 1990, 29, 329-343.

(16) Buttry, D. A. In *Electrochemical Interfaces*; Abruna, H. D., Ed.; VCH Publishers: New York, 1991, pp 531-566.

(17) Ebersole, R. C.; Ward, M. D. *J. Am. Chem. Soc.* 1988, 110, 8623-8628.

(18) Ebersole, R. C.; Foss, R. P.; Ward, M. D. *Bio/Technology* 1991, 9, 450-454.

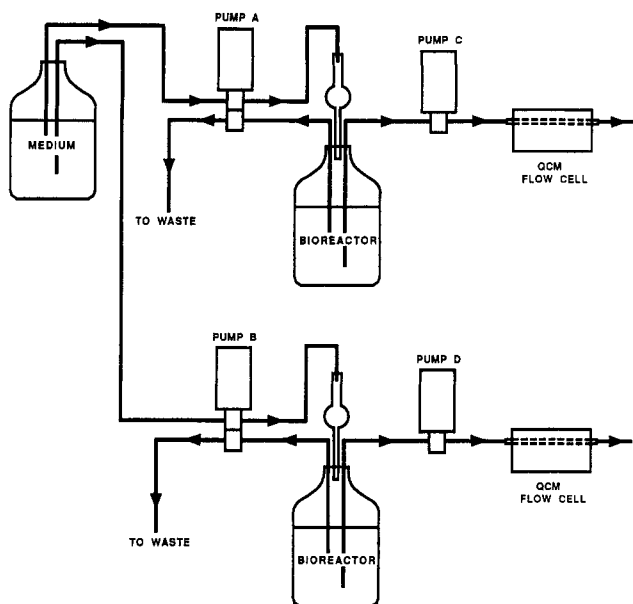


**Figure 1.** Diagram of flow system showing the direction of flow. Pumps A and B control the dilution rate in the bioreactors, and pumps C and D control the flow rate into the QCM flow cell.

*Pseudomonas cepacia*, which is a common contaminant in ultrapure water systems. This study was designed to simulate a microbial contamination event in a sterile water system. Microbial adhesion experiments involved long-term monitoring of frequency signals from quartz resonators and required strategies to eliminate signals due to random fluctuations in environmental parameters such as temperature and pressure.

## EXPERIMENTAL SECTION

**Bacterial Strain.** *P. cepacia* (25416) was obtained from the American Tropic Culture Collection (Rockville, MD). Stock cultures were maintained on nutrient agar slants and stored at  $-70^{\circ}\text{C}$  in nutrient broth with 25% glycerol.

**Growth Medium.** The growth medium contained  $5.7 \times 10^{-6}$  M  $\text{K}_2\text{PO}_4$ ,  $5.5 \times 10^{-6}$  M glucose,  $4.6 \times 10^{-6}$  M  $\text{NH}_4\text{Cl}$ ,  $1.0 \times 10^{-6}$  M  $\text{MgSO}_4$ ,  $3.0 \times 10^{-7}$  M  $\text{CaCl}_2$ ,  $2.1 \times 10^{-7}$  M  $\text{NaCl}$ , and a dilute Wolfe's mineral solution<sup>19</sup> ( $9 \times 10^{-8}$  M nitrilotriacetic acid,  $1.2 \times 10^{-8}$  M  $\text{MnSO}_4$ ,  $4 \times 10^{-9}$  M  $\text{FeSO}_4$ ,  $4 \times 10^{-9}$  M  $\text{CoSO}_4$ ,  $4 \times 10^{-9}$  M  $\text{ZnSO}_4$ ,  $2 \times 10^{-9}$  M  $\text{H}_3\text{BO}_3$ ,  $5 \times 10^{-10}$  M  $\text{CuSO}_4$ ,  $6 \times 10^{-10}$  M  $\text{NaSeO}_4$ , and  $5 \times 10^{-10}$  M  $\text{NaMoO}_4$ ) in 18 M $\Omega$ -cm water. The final solution was titrated to pH 7.2. All chemicals were reagent-grade. The medium was sterilized with a 0.2- $\mu\text{m}$  pore size filter.

**Flow System.** The flow system consisted of a medium reservoir, two constant-volume stirred bioreactors, two stainless steel heat exchange tubes (0.64-cm outer diameter), two flow cells, silicone tubing, four pumps, and two waste reservoirs (Figure 1). The 500-mL bioreactors were outfitted with an inlet drip tube, an exit line, an air stone, a stir bar, and a vent. The drip tube provided discontinuous flow which prevented microbial back-contamination of the medium reservoir. The exit line was positioned to maintain the volume of the flask at 350 mL. The flow rate into and out of the bioreactors was controlled with pumps A and B and was approximately 3.5 mL/min. The flow rates through the flow cells, which were controlled with pumps C and D, ranged from 2.4 to 3.2 mL/min. Because *P. cepacia* is a strict aerobe, the bioreactor fluid was stirred and sparged with air. Each flow cell was constructed from a block of Delrin (20 cm in length by 10 cm in width by 7.6 cm in thickness) cut into two sections. One section of the block was milled to form the flow channel and contained a resistance temperature detector (RTD), while a 2.54-cm-diameter AT-cut quartz crystal was sealed with silicone glue into the other section. The two sections were

sealed with a silicone gasket and bolted together. The volume of the flow cell was approximately 30 mL. The flow cells were sterilized by ethylene oxide, while the rest of the flow system was autoclaved (20 psi and  $120^{\circ}\text{C}$  for 25 min). The waste lines exited into a constant volume overflow tube that was housed within a sterile reservoir. The overflow tube was located approximately 1 m above the flow cell to maintain stable back-pressure on the flow cell.

**QCM Analysis.** Both sides of 5-MHz AT-cut quartz crystals (Valpey-Fischer, Hopkinton, MA) were coated with approximately 1000 Å of chromium followed by 2500 Å of gold in a keyhole pattern of different radii. A gold surface with a radius of 3 mm was exposed to air and a gold surface with a radius of 5 mm was exposed to the aqueous environment. Wires soldered onto the gold electrodes provided the electrical connection to the oscillator boards that were contained within Al boxes mounted onto the flow cells. Eight 9-V batteries connected in parallel provided power for up to 16 days. A voltage regulator chip provided a stable 5-V input signal. The oscillation frequency was measured at 5-min intervals by a dual-channel 775A frequency counter (Keithley Instruments, Cleveland, OH). Resistance measurements, also taken at 5-min intervals, were performed with a Keithley 196 digital voltmeter and 705 scanner to determine the temperature in the flow cell. The QCM flow cells and the heat-exchange tubing were placed in a Faraday cage/constant temperature box ( $\pm 0.15^{\circ}\text{C}$ ), and the entire flow system was housed in a constant temperature room ( $\pm 0.3^{\circ}\text{C}$ ).

An Asyst (Rochester, NY) program was written to control data acquisition through a general-purpose interface bus. In addition, Asyst was used to convert the frequency shift data into cell count data, differentiate the cell count data, and smooth the differentiated data using a low-pass Blackman filter with a cut-off frequency of  $1\text{ h}^{-1}$ .

**Experimental Procedures.** Studies were performed to establish the magnitude of the frequency shifts associated with pressure and temperature changes. Temperature studies were performed in the flow cell under no-flow conditions. The frequency response was monitored as the bath temperature was increased at 0.2 and 0.3  $^{\circ}\text{C}$  intervals from 22 to 28  $^{\circ}\text{C}$  and subsequently returned to 22  $^{\circ}\text{C}$ . The temperature of the solution was monitored with the RTD. The exit line was vented to atmospheric pressure.

In the pressure-response experiments, pressure was controlled by a needle valve downstream of the flow cell and monitored with pressure gauges. An upstream pump recirculated water through the system at a flow rate of 3.2 mL/min using reinforced high-pressure silicone tubing. The pressure was increased, and the observed pressure and frequency shift was recorded. The observed frequencies were referenced to the frequency in the flow cell with the needle valve completely open. The temperature was maintained at  $25.00 \pm 0.15^{\circ}\text{C}$ .

In the microbial biofilm experiment, stability tests were performed prior to the start of the experiments. The first test examined the short-term stability of the frequency signal in air. If it remained stable within  $\pm 0.5$  Hz over a 5-min interval, the medium was pumped into the bioreactors and subsequently into the flow cells at flow rates ranging from 2.4 to 3.2 mL/min. The flow through the flow cell was calculated to be laminar with a worst case Reynolds's number of 30. Constant drift (1–3 Hz/h) was usually associated with new quartz resonators. This drift may be associated with chemical modifications of the gold surface, such as gold oxidation and chemical adsorption. Within 24 h, the temperature of the flow system equilibrated, and a 24-h culture containing actively growing bacteria was inoculated into the bioreactor. The number of bacteria in the inoculum was determined by acridine orange epi-fluorescent microscopy (described below). After inoculation, the biofouling event was monitored by the QCM. At the end of each experiment, the number of bacteria in the liquid phase and the number of cells attached to the surface were determined.

**Bacterial Cell Counts.** The number of bacteria in the inoculum, liquid phase, and biofilm were determined by an acridine orange (dibenzo[b,e]pyridine) staining procedure utilizing stained black Nuclepore filters (Costar, Cambridge, MA).

(19) Balch, W. E.; Fox, G. E.; Nagrum, L. J.; Woese, G. R.; Wolfe, R. S. *Microbiol. Rev.* 1979, 43, 260–296.

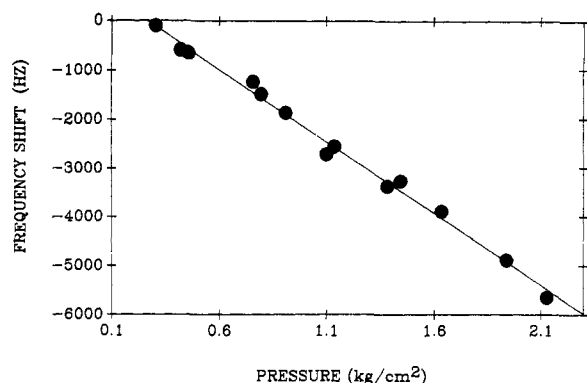


**Figure 2.** Plot of the frequency shift of a 5-MHz AT-cut quartz crystal with pressure change at a flow rate of 4 mL/min and  $25.0 \pm 0.15$  °C. The data can be fit to a linear function with the equation,  $y = 2940x + 781$  ( $r^2 = 0.997$ ).

The AO counting method<sup>20</sup> is commonly used in microbiology to estimate biomass and was the method of choice in these experiments because no other methods that estimate biomass have low enough detection limits. The staining procedure involved transferring an aliquot of a bacterial cell suspension to the filter apparatus and subsequent addition of 2 mL of a  $2.7 \times 10^{-4}$  M acridine orange solution. After approximately 3 min, the filter was removed, dried, placed on a drop of immersion oil, and visualized with a microscope equipped with a 100-W mercury vapor source and epi-fluorescent collection optics (Nikon, Garden City, NJ). Twenty-five microscopic fields (100 by 100  $\mu\text{m}$ ) were counted, and the mean and standard deviation of the cell counts were determined.

Direct counting of bacteria on the gold surface was not possible because *P. cepacia* grows in colonies on surfaces. Biofilm bacteria were fixed by replacing the medium with 2.5% glutaraldehyde in 0.1 M phosphate buffer (pH 7.2). After fixation, a 2.8-cm-diameter plastic tube and a silicone gasket were placed around the quartz crystal, and 10 mL of sterile phosphate solution was added. The solution was sonicated for 10 s at 15 W to remove the bacteria from the surface. The quartz crystals were examined after sonication to ensure complete removal. The bacterial suspension was transferred to the filter apparatus, stained, and counted.

**Scanning Electron Microscopy.** Biofilm microorganisms attached to the quartz resonators were fixed in 2.5% glutaraldehyde in 0.1 M potassium phosphate buffer for 30 min. The crystals were removed from the flow cells, dried with a series of acetone/water solutions, and postfixed with osmium tetroxide. Following evaporation of 100 Å of gold/palladium alloy, the sample was examined using an ETEC Autoscan microscope.

## RESULTS AND DISCUSSION

**Pressure Effects.** Elevated pressures were investigated because these conditions would be encountered in water systems. The frequency of the QCM in our experiments proved to be more sensitive to pressure changes than those reported for QCM's exposed to vacuum or air. Using a QCM to monitor the mass of particles suspended in the atmosphere, Olin and Sems reported that ambient fluctuations of  $\pm 0.07$   $\text{kg}\cdot\text{cm}^{-2}$  caused a frequency shift of less than 1 Hz.<sup>21</sup> However, we found that the frequency shift data for a given increase in hydraulic pressure fit a linear function ( $r^2 = 0.996$ ) with a slope of  $-2970$   $\text{Hz}\cdot\text{cm}^{-2}\cdot\text{kg}^{-1}$  for pressure increased to  $+2.1$   $\text{kg}\cdot\text{cm}^{-2}$  (Figure 2).

The increased sensitivity of the QCM to pressure changes can be traced to the manner in which the pressure was applied in our experiments. One side of the crystal was exposed to hydrostatic pressure, while the other side remained at

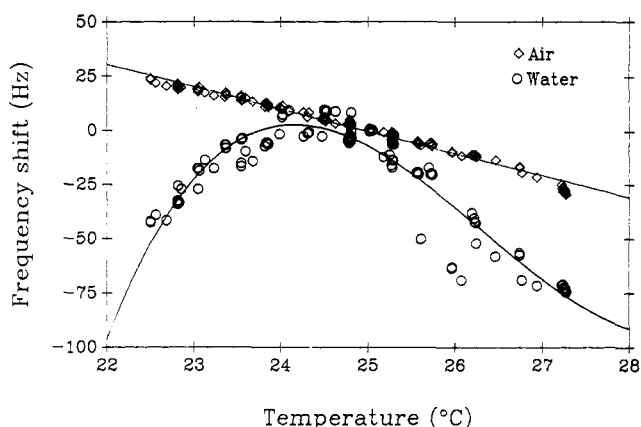


**Figure 3.** Comparison of the frequency shift versus temperature for a stressed AT-cut quartz crystal exposed to sterile water under no-flow conditions at ambient pressures (O) and an unstressed crystal in air ( $\diamond$ ).

atmospheric pressure. For pressure increases on one side of the crystal, Heusler et al. found that the relationship between pressure and frequency shift was parabolic when pressure was varied from  $+0.12$  to  $-0.12$   $\text{kg}\cdot\text{cm}^{-2}$ .<sup>22</sup> A  $+0.12$   $\text{kg}\cdot\text{cm}^{-2}$  pressure increase produced approximately a  $-175$ -Hz shift. It was suggested that increasing the hydrostatic pressure on one side of the crystal results in a distortion in the crystal which in turn produces the frequency shift.

**Temperature Effect.** The effect of temperature on the oscillation frequency has been documented for AT-cut quartz crystals, where the temperature coefficient for an AT-cut quartz crystal at 25 °C is typically about  $0.05$   $\text{ppm}\cdot\text{C}^{-1}$ , and the temperature response can be fit to a third-order equation.<sup>23</sup> However, when the 5-MHz AT-cut quartz crystals are sealed into a flow cell and one side of the crystal is exposed to water, the temperature response is dramatically changed (Figure 3). For temperatures ranging between 22 and 28 °C, the frequency response of the crystals can be represented by a linear function in air and a parabolic function for a quartz crystal sealed into a flow cell and filled with water (no flow). Zero hertz was arbitrarily assigned to 25.000 °C. Increased temperature responses for crystals sealed in a flow cell and exposed to water have also been reported by Buttry<sup>16</sup> who suggested that this effect could be attributed to viscosity and density changes associated with pure water at increased temperatures. However, increasing the temperature from 20 to 30 °C produces a monotonic decrease in water density from  $0.998$  to  $0.996$   $\text{g}\cdot\text{cm}^{-3}$  and monotonic increase in viscosity from  $1.0020$  to  $0.7975$  cP.<sup>24</sup> Thus, density and viscosity changes do not explain the parabolic nature of this curve. As with the pressure response, it can be hypothesized that the hydraulic pressure caused mechanical stress on the crystal sealed in a flow cell, which in turn altered the temperature response of the crystal. In order to avoid frequency shifts caused by temperature fluctuations, the temperature was maintained at  $25.00 \pm 0.15$  °C.

**Effects of Microbial Biofilms.** Tests were performed to ascertain the stability of the QCM under sterile conditions with constant temperature and pressure. The measured frequency shift resulting from the introduction of sterile medium into the flow cell was  $-2028 \pm 241$  Hz. A value of  $-670$  Hz is calculated using the relationship derived by Gordon and Kanazawa for viscous over layers.<sup>25</sup> The discrepancy in

(22) Heusler, K. E.; Grzegorzewski, A.; Jackel, L.; Pietrucha, J. *Ber. Bunsen-Ges. Phys. Chem.* 1988, 92, 1218-1225.

(23) *Application of Piezoelectric Quartz Crystal Microbalance*; Lu, C., Czanderna, A., Eds.; Elsevier: New York, 1984.

(24) *Handbook of Chemistry and Physics*; Weast, R. C., Astle, M. J., Beyer, W. H., Eds.; CRC Press, Inc.: Boca Raton, FL, 1988.

(20) Hobbie, J. E.; Daley, R. J.; Jasper, S. *Appl. Environ. Microbiol.* 1977, 33, 1225-1228.

(21) Olin, J. G.; Sems, G. J. *Atmos. Environ.* 1971, 5, 653-668.

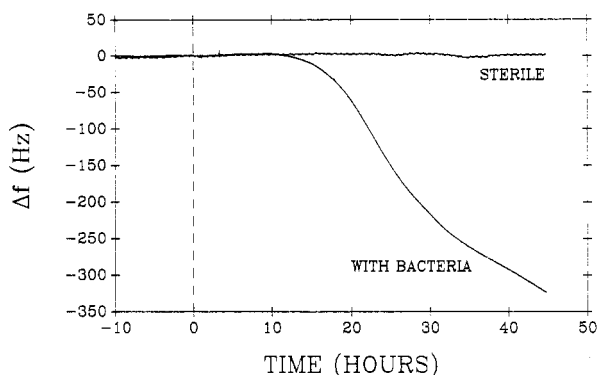


**Figure 4.** Graph comparing the frequency response of the QCM monitoring a sterile flowing medium versus biofilm formation. Inoculation time is at time zero, and the frequency at the inoculation time was arbitrarily set to 0.0 Hz.

these results is caused in part by the hydrostatic pressure in the flow cell. A stable frequency was monitored for a 54-h interval and the long-term drift noise was  $\pm 4.0$  Hz (Figure 4). In addition, the short-term noise was less than 0.5 Hz for a given 5-min interval.

Figure 4 compares the frequency shift data for a flow system inoculated with *P. cepacia* cells with the frequency data of the sterile control. In this graph, negative time represents the stabilization period following the introduction of water and prior to inoculation at time zero. In the experiment of Figure 4, 3 mL of a culture containing  $(7 \pm 3) \times 10^7$  bacteria·mL<sup>-1</sup> was inoculated into a bioreactor. The dead volume of the tubing was approximately 70 mL, and the flow rate was 2.4 mL/min, thus unretained substances should arrive in the flow cell in approximately 30 min. However, the frequency did not decrease until approximately 10 h. The delay probably resulted from adsorption of the inoculum-bacteria to surfaces upstream of the flow cell and only a few inoculum-bacteria (less than the detection limit) attached to the quartz resonator. In an ancillary experiment performed in flasks, most *P. cepacia* cells in the liquid phase adsorbed to the side of the flasks within minutes (result not shown). The attachment event has been described as a two-step process: reversible adsorption followed by irreversible chemisorption possibly facilitated by extracellular polymers, organelles, or fimbriae.<sup>1</sup> Therefore, inoculum-bacteria must desorb or produce daughter cells to generate liquid-phase cells that can adsorb downstream onto the quartz resonator.

Attached bacteria utilize adsorbed nutrients<sup>26</sup> and/or nutrients from the bulk phase, replicate, and form colonies. The negative frequency shift after 10 h results mainly from surface growth of the attached bacteria. However, a portion of the signal also may result from viscosity and density changes in the solution at the QCM interface caused by actively growing bacteria or biomass from newly adsorbed liquid-phase bacteria. As the biomass increases, the frequency continues to decrease. After a -325-Hz frequency shift, the surface density of microorganisms was determined to be  $3.3 \times 10^7$  cells·cm<sup>-2</sup> by the AO counting procedure. *P. cepacia* cells are rod shaped with an approximate length of 1  $\mu$ m and a width of 0.5  $\mu$ m. Thus, the surface coverage of the bacteria is calculated to be approximately 17%.

Similar experiments were stopped at different frequency shifts, and the number of bacteria on the surface were determined. The calibration curve of measured frequency shift versus the number of *P. cepacia* cells within the biofilm matrix is presented in Figure 5. The relationship between biofilm cell counts and frequency shift is monotonic for 2

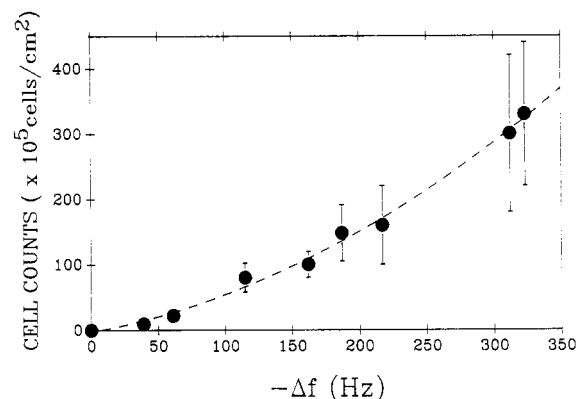


**Figure 5.** Plot of the number of attached bacteria within a biofilm versus frequency shift. Empirically, the plot can be fit to a second-order equation (eq 1,  $r^2 = 0.995$ ).

orders of magnitude but not linear. Empirically, the plot can be represented by a parabolic function ( $R^2 = 0.995$ ) with the equation

$$N_c = -2.84 + 0.37|\Delta f| + 0.002|\Delta f|^2 \quad (1)$$

where  $N_c$  is  $10^5$  cells·cm<sup>-2</sup> and  $\Delta f$  is the frequency shift. A conservative estimate of the limits of detection were calculated from the equation for the curve and the long-term drift noise. The detection limit was determined to be  $3 \times 10^5$  *P. cepacia* bacteria·cm<sup>-2</sup>.

A comparison of the precision of the cell counts and frequency measurements is of interest. The AO cell counting method typically has large relative errors resulting from nonuniform surface coverage of bacteria on the filters.<sup>20</sup> The QCM frequency shifts, on the other hand, are very precise: 5-MHz frequency signals were measured to 0.01-Hz accuracy and long-term drift noise was  $\pm 4$  Hz.

The nonlinearity of the calibration curve may be attributed to microbiological effects such as (1) colony formation, (2) cell shrinkage, and (3) extracellular polymer production. Scanning electron and AO epi-fluorescent microscopy showed that *P. cepacia* cells tend to remain closely packed in colonies that were evenly distributed on the surface of the resonator. Moreover, growth within the colonies is longitudinal along the solid/liquid interface, and larger colonies contained cells that do not contact the surface (Figure 6). This type of contiguous colonization behavior has been observed by computer-enhanced microscopy for *Pseudomonas fluorescens*.<sup>27</sup> It can be hypothesized that the shear wave, which in water penetrates approximately 2500 Å,<sup>25</sup> may not propagate far enough into nonrigid biofilms to detect bacteria not contacting the surface. The acoustic properties of a *P. cepacia* cell are unknown and may not remain constant. Secondly, bacteria within biofilms on densely populated portions of the surfaces (colonies) could decrease in size due to nutrient limitation, thus increasing the number of bacteria per unit biomass. Bacteria decrease in size under nutrient limited conditions.<sup>28</sup> Finally, bacteria produce extracellular polymers that may alter the viscoelastic properties of biofilms which in turn effects the frequency response. For example, *Pseudomonas atlantica* produces extracellular polymers in response to physiological stress.<sup>29</sup> These extracellular poly-

(27) Lawrence, J. R.; Delaquis, P. J.; Korber, D. R. *Microb. Ecol.* 1983, 14, 1.

(28) Humphrey, B.; Kjelleberg, S.; Marshall, K. C. *Appl. Environ. Microbiol.* 1983, 45, 43.

(29) Uhlinger, D. J.; White, D. C. *Appl. Environ. Microbiol.* 1983, 45, 64.

(30) Sauerbrey, G. Z. *Phys.* 1959, 155, 206.

(31) Miller, J. G.; Bolef, D. I. *J. Appl. Phys.* 1968, 39, 4589.

(32) Lu, C.; Lewis, O. *J. Appl. Phys.* 1972, 43, 4385.

(25) Gordon, J. G.; Kanazawa, K. K. *Anal. Chem.* 1985, 57, 1770.

(26) Power, K.; Marshall, K. C. *Biofouling* 1988, 1, 163.

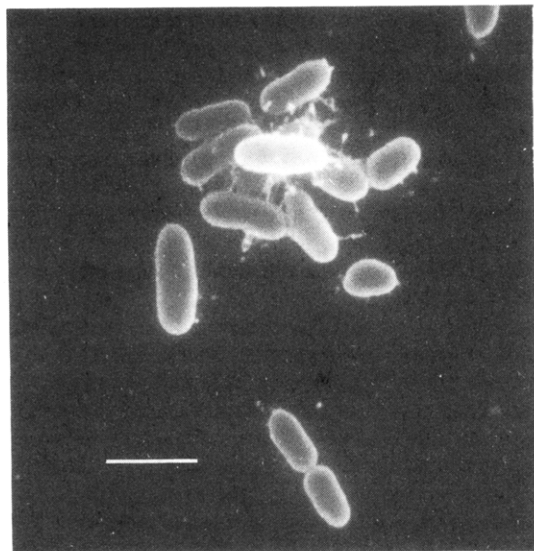


**Figure 6.** Electron micrograph showing colony formation on the oscillating gold surface of a QCM. *P. cepacia* tends to colonize the surface along the solid/liquid interface but eventually forms layers that do not contact the surface. The filamentous substance is assumed to be extracellular polymers. The bar equals 1  $\mu\text{m}$ .

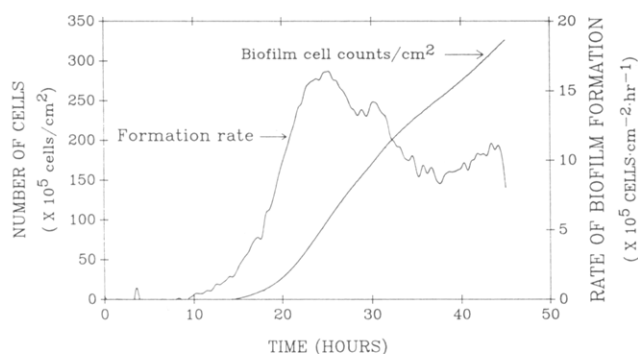


**Figure 7.** Graph presenting the cell count data versus time as predicted by eq 1 for the data shown in Figure 4 (left axis). The graph also shows the first derivative of the cell counts versus time data (right axis). This first derivative plots shows the instantaneous rate of biofilm formation versus time.

mers act as molecular bridges creating chemical bonds, dipole interactions, and/or hydrophobic interactions between the surface and the microbes present in the biofilm.<sup>3</sup> Evidence for the existence of extracellular polymer in colonies and mature *P. cepacia* biofilms has been observed in electron micrographs where the polymers have collapsed in preparation and appear as filaments (Figure 6).

(33) Ingraham, J. L.; Maaloe, O.; Neidhardt, F. C. *Growth of the Bacterial Cell*; Sinauer Associates, Inc.: Sunderland, MS, 1983; p 3.

The calibration curve (Figure 5) was also used to predict the number of bacteria attached to the oscillating gold surface. Using the empirically derived equation for the calibration curve, the frequency shift curve from Figure 4 was converted into bacterial counts per unit area curve (Figure 7). From these data, the first derivative of the bacterial count data with respect to time was generated to determine the replication/attachment rate of bacteria within the biofilm. From Figure 7, the rate of biofilm formation increased dramatically at 10 h and achieved a maximum rate of  $1.7 \times 10^6$  cells·cm<sup>-2</sup>·h at approximately 25 h.

Mathematical models for conversion of  $\Delta f$  into mass have been derived.<sup>30-32</sup> Sauerbrey developed an equation that directly relates the  $\Delta f$  to the mass load but assumes that the shear modulus of the attached layer is the same as quartz.<sup>30</sup> Relating  $\Delta f$  to biofilm-biomass is inappropriate because nonrigid living biofilms violate this assumption. Nonetheless, application of the Sauerbrey equation and eq 1 at the frequency shift corresponding to the detection limit gave an estimate of the wet mass of a single attached *P. cepacia* cell of 0.8 pg, which is comparable to the literature values of 1 pg obtained for an *Escherichia coli* cell grown on rich medium.<sup>33</sup> Frequency conversion models other than the Sauerbrey theory are more appropriate for viscoelastic layers but require prior knowledge of the acoustic properties of the adsorbed layers. Little is known about the viscoelastic properties of biofilms, but it would seem likely that these properties are dynamic and change with the physiological status of the bacteria within a biofilm.

In summary, the results presented here demonstrate that the QCM methodology can monitor sterile aqueous environments for days. Thus, it may be possible to use the QCM as an extremely sensitive remote sensing device for microbial contamination in ultrapure water systems. In addition, these results were consistent with the general knowledge of biofilm formation. The technique can also monitor the rate of biofilm formation. Future experiments will consider the effect of varying surface and liquid-phase chemistry on biofilm formation and will attempt to employ temperature and pressure compensation methods.

#### ACKNOWLEDGMENT

The research was supported by the National Aeronautics and Space Administration (NAS8-38493), the National Science Foundation (CHE-8718057), and the Office of Navy Research (N00014-88-k-0012). The oscillation board was a gift of Owen B. Melroy, IBM, San Jose, CA. The authors thank C. Dial, J. Sniatecki, and J. Stafford for their respective contributions.

RECEIVED for review July 17, 1992. Accepted October 16, 1992.